Effect of coupling of forward- and backward-going electron-hole pairs on the static local-field factor of jellium

Argyrios Tsolakidis,[1] Eric L. Shirley,[2] and Richard M. Martin[1]
[1]*Department of Physics and Materials Research Laboratory, University of Illinois at Urbana-Champaign, Urbana, Illinois 61801, USA*
[2]*Optical Technology Division, Physics Laboratory, National Institute of Standards and Technology, Gaithersburg, Maryland 20899-8441, USA*

(Received 10 February 2003; revised manuscript received 31 July 2003; published 15 January 2004)

We investigate the effect of the coupling of the forward- and backward-going electron-hole pairs on the static local-field factor of jellium with and without a gap. We calculate the static local-field factor for the two types of jellium as a function of **q** using the Bethe-Salpeter equation. We assume that a particle and a hole interact via a statically screened Coulomb interaction. The polarization diagrams that include this interaction are summed to infinite order, leading to a matrix equation for the inverse of the polarization propagator. Employing a string of manipulations we convert the matrices in convenient forms, and we then invert the resulting matrices iteratively. This allows us to use matrices of very large size, something that would have not been feasible with straightforward inversion, and therefore achieve a very high level of convergence of results with respect to sampling of electron states in the Fermi sea with relative computational ease. For the calculation of the static local-field factor, we find that the coupling of both kinds of pairs gives qualitatively different results compared to the case when there is no coupling, and that the coupling of both kinds of electron-hole pairs is necessary for obtaining the most accurate results. We compare our results with recent calculations and point out the similarities and differences.

DOI: 10.1103/PhysRevB.69.035104 PACS number(s): 78.20.−e

I. INTRODUCTION

Various researchers[1–7] using the Bethe-Salpeter equation for solids either ignore the backward-going electron-hole pairs or do not couple the forward- and backward-going electron-hole pairs. Recently Olevano and Reining[8] in their calculation of the electron energy-loss spectrum of silicon included both kinds of electron-hole pairs and treated their coupling as a perturbation. Their results are in excellent agreement with the experiment.[9] The main motivation of this work is to study the effect of the coupling of forward- and backward-going electron-hole pairs on the static local-field factor of jellium with and without a gap. Jellium with a gap is a model of an insulator as a free electron gas with a gap at the Fermi energy.[10] The effect of the coupling in jellium suggests the corresponding effect in solids.

The local-field factor $G(|\mathbf{q}|)$ was introduced by Hubbard[11] in his attempt to include the contribution of exchange into the proper polarizability of the electron gas, $\chi(\mathbf{q},\omega)$, where $\mathbf{q}$ and ω are the polarization's wave vector and frequency.

Hubbard, by employing some approximations, was able to sum an infinite series of ladder diagrams. The resulting form of the proper polarizability was given by the following expression:

$$\chi_H(\mathbf{q},\omega)=\frac{\chi_{RPA}(\mathbf{q},\omega)}{1+v_c(|\mathbf{q}|)G(|\mathbf{q}|)\chi_{RPA}(\mathbf{q},\omega)}, \tag{1}$$

with

$$G(|\mathbf{q}|)=\frac{|\mathbf{q}|^2}{2(|\mathbf{q}|^2+|\mathbf{q}_F|^2)}, \tag{2}$$

and $v_c(|\mathbf{q}|)=4\pi e^2/|\mathbf{q}|^2$ being the Fourier transform of the Coulomb interaction. In the above equations, $\chi_{RPA}(\mathbf{q},\omega)$ is the random-phase approximation (RPA) proper polarizability and $\mathbf{q}_F$ is the Fermi wave vector. Because Hubbard only included certain exchange diagrams in his calculation of the proper polarizability for jellium, the local-field factor he introduced accounts only for the exchange hole around each electron. A number of authors[12–15] have tried to include the Coulomb correlation empirically by including a dimensionless parameter ξ into Eq. (2):

$$G(|\mathbf{q}|)=\frac{|\mathbf{q}|^2}{2(|\mathbf{q}|^2+\xi|\mathbf{q}_F|^2)}. \tag{3}$$

Although much more elaborate calculations of the proper polarizability of the electron gas were done over the years,[15–41] most of them have the form of Eq. (1), introduced by Hubbard.

This paper is organized as follows: In Sec. II, we describe the method of calculation and give details about some subtle points of our calculation. In Sec. III we present the results for the static local-field factor of the electron gas, with and without a gap, for the case where both kinds of electron-hole pairs are coupled and for the case where they are not coupled. We discuss and compare our results with the ones obtained from other calculations. In Sec. IV we present our conclusions.

II. METHOD OF CALCULATION

A. Jellium

The static local-field factor is important because it is related to the exchange-correlation factor $f_{xc}(|\mathbf{q}|)$ and conse-

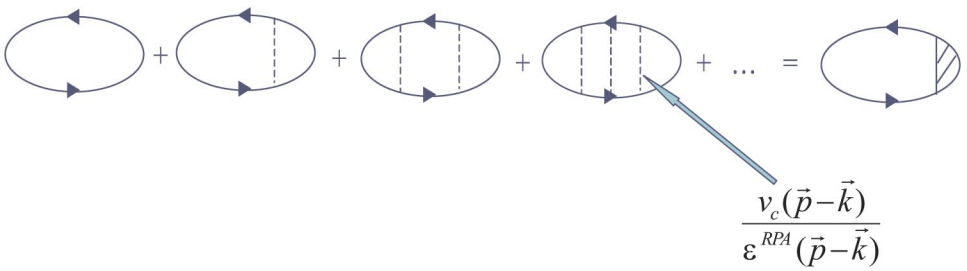

FIG. 1. Diagrams contributing to the calculation of the proper polarizability.

quently to the exchange-correlation energy $E_{xc}[n]$, a quantity of great importance in density-functional theory:[42,43]

$$G(|\mathbf{q}|) = -\frac{f_{xc}(|\mathbf{q}|)}{v_c(|\mathbf{q}|)} = \frac{1}{v_c(|\mathbf{q}|)}\left(\frac{1}{\chi(\mathbf{q})} - \frac{1}{\chi_{RPA}(\mathbf{q})}\right). \quad (4)$$

Throughout this work, suppressing a frequency argument denotes the static value for a constant, e.g., $\chi(\mathbf{q}) = \chi(\mathbf{q}, \omega = 0)$. $E_{xc}[n]$ and $f_{xc}(|\mathbf{q}|)$ are directly related in real space:

$$f_{xc}(|\mathbf{r}-\mathbf{r}'|) = \left[\frac{\delta^2 E_{xc}[n]}{\delta n(\mathbf{r})\,\delta n(\mathbf{r}')}\right]_{n_0}. \quad (5)$$

In our approach, we calculate the proper polarizability of the electron gas, $\chi(\mathbf{q})$, at a certain level of approximation, and, by using Eq. (4), we obtain $G(|\mathbf{q}|)$. For the calculation of the proper polarizability, we only include diagrams where the electron and the hole interact via a statically screened Coulomb interaction, and we sum these diagrams to infinite order. We show the diagrams included and their summation in Fig. 1. Here we use a noninteracting, time-ordered electron Green's function,

$$G^0(p) = \frac{1}{E - |\mathbf{p}|^2/2 \pm i\eta}, \quad (6)$$

which implies that $G(|\mathbf{q}|) = 0$ gives the RPA result, and allows for a qualitative assessment of the significance of coupling forward- and backward-going electron-hole pairs. We henceforth make the abbreviation, $E(\mathbf{p}) = |\mathbf{p}|^2/2$. Here we use four-vector notation, i.e., we have $p = (\mathbf{p}, E)$, $q = (\mathbf{q}, \omega)$, etc. Therefore, all electron states with momentum smaller than the Fermi momentum q_F, i.e., $|\mathbf{p}| < q_F$, are filled in the ground state, and all states with $|\mathbf{p}| > q_F$ are empty in the ground state. The occupancy of a state, $f(\mathbf{p})$, is therefore given by $f(\mathbf{p}) = 1$ for $|\mathbf{p}| < q_F$ and $f(\mathbf{p}) = 0$ for $|\mathbf{p}| > q_F$. Also, this work assumes that one has zero temperature. From Feynman rules,[44] one finds that the proper polarizability $\chi(q)$ can be expressed in a compact way in terms of the irreducible vertex function $\Gamma(p, p+q)$:

$$\chi(q) = -2i\int \frac{d^4p}{(2\pi)^4} G^0(p) G^0(p+q) \Gamma(p, p+q). \quad (7)$$

The factor of 2 in Eq. (7) comes from the summation over spins. Use of the statically screened interaction between the electron and the hole has as a consequence the suppression of the dependence of χ on the energy exchanged between the electron and the hole. Therefore $\Gamma(p, p+q)$ only depends on ω, the total energy of the electron-hole pair, which in our case is equal to zero because we calculate the static proper polarizability $\chi(\mathbf{q})$. This allows us to perform the internal frequency summation in Eq. (7) without any difficulty. The static screening of the Coulomb interaction and the choice of the diagrams that contribute to the static proper polarizability $\chi(\mathbf{q})$ are the most important approximations employed for the calculation of the static local-field factor $G(|\mathbf{q}|)$. Because of the lack of dependence of $\Gamma(p, p+q)$ on the internal frequency, Eq. (7) takes the form

$$\chi(\mathbf{q}) = -2i\int \frac{d^4p}{(2\pi)^4} G^0(p) G^0(p+q) \Gamma(\mathbf{p}, \mathbf{p}+\mathbf{q}). \quad (8)$$

A pictorial representation of the static proper polarizability $\chi(\mathbf{q})$ is given in Fig. 2.

The equation of motion for the irreducible vertex function $\Gamma(\mathbf{p}, \mathbf{p}+\mathbf{q})$ is

$$\Gamma(\mathbf{p}, \mathbf{p}+\mathbf{q}) = \delta_{\mathbf{q},0} - i\int \frac{d^4k}{(2\pi)^4} \frac{v_c(\mathbf{p}-\mathbf{k})}{\epsilon^{RPA}(\mathbf{p}-\mathbf{k})} G^0(k) \times G^0(k+q) \Gamma(\mathbf{k}, \mathbf{k}+\mathbf{q}). \quad (9)$$

Equation (9) is depicted in terms of Feynman diagrams in Fig. 3. We perform the internal frequency summation in Eq. (9), and we convert the integration in k space into summation over discrete $\mathbf{k}$ points. The equation for $\Gamma(\mathbf{p}, \mathbf{p}+\mathbf{q})$ takes the form

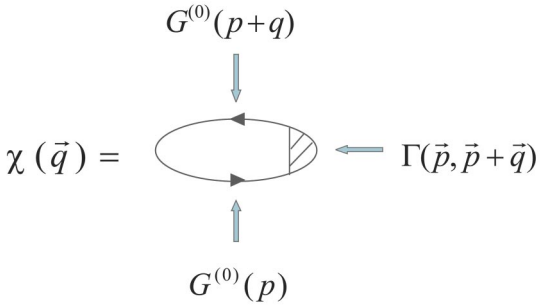

FIG. 2. Static proper polarizability.

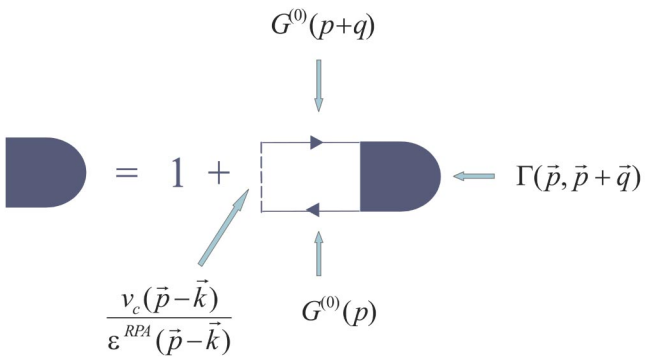

FIG. 3. Diagrammatic representation of the irreducible vertex function.

$$\Gamma(\mathbf{p},\mathbf{p}+\mathbf{q})=\delta_{\mathbf{q},0}+\frac{1}{V}\sum_{\mathbf{k}}\frac{v_c(\mathbf{p}-\mathbf{k})}{\epsilon^{RPA}(\mathbf{p}-\mathbf{k})}\frac{f(\mathbf{k})-f(\mathbf{k}+\mathbf{q})}{E(\mathbf{k})-E(\mathbf{k}+\mathbf{q})+i\eta}\times\Gamma(\mathbf{k},\mathbf{k}+\mathbf{q}). \tag{10}$$

V is the volume of the finite-sized ''box'' appropriate for one's discretization of values of $\mathbf{k}$. We next define the matrices

$$W_{\mathbf{pk}}=\frac{v_c(\mathbf{p}-\mathbf{k})}{\epsilon^{RPA}(\mathbf{p}-\mathbf{k})} \tag{11}$$

and

$$F_{\mathbf{kk}'}=\frac{1}{V}\frac{f(\mathbf{k})-f(\mathbf{k}+\mathbf{q})}{E(\mathbf{k})-E(\mathbf{k}+\mathbf{q})+i\eta}\delta_{\mathbf{kk}'}. \tag{12}$$

Using all of the above definitions, Eq. (10) can be expressed in matrix form, suppressing all indices, as follows:

$$\Gamma=1+WF\Gamma=F^{-1}(F^{-1}-W)^{-1}. \tag{13}$$

Here, these matrices act in a space in which a vector has one component corresponding to each possible electron-hole pair state. In the same way we can write Eq. (8), the equation for the static proper polarizability $\chi(\mathbf{q})$, using

$$\chi(\mathbf{q})=2V\langle\Phi|F\Gamma|\Phi\rangle, \tag{14}$$

where Φ is one such vector with components all equal to $1/\sqrt{V}$. We combine Eqs. (13) and (14) to obtain the final form of the equation for the static proper polarizability,

$$\chi(\mathbf{q})=2V\langle\Phi|(F^{-1}-W)^{-1}|\Phi\rangle. \tag{15}$$

As mentioned, one of the most important aspects of our calculation is the coupling of both forward- and backward-going electron-hole pairs. A forward-going electron-hole pair is the electron-hole pair for which we have $E(\mathbf{k})-E(\mathbf{k}+\mathbf{q})>0$, while a backward-going electron-hole pair is the one for which we have $E(\mathbf{k})-E(\mathbf{k}+\mathbf{q})<0$. According to Eq. (15), in order to calculate $\chi(\mathbf{q})$ we subtract the statically screened Coulomb interaction matrix W from the inverse of the free electron-hole propagator matrix F^{-1}, and we invert the resulting matrix. During the inversion, matrix elements of W can couple forward- and backward-going electron-hole pairs to both kinds of pairs, although coupling opposite types of pairs can be of secondary importance and has often been neglected because of resulting simplifications.

For the calculation of the static proper polarizability $\chi(\mathbf{q})$ and consequently the local-field factor $G(|\mathbf{q}|)$, we create a cubic grid of k points. The dimensions of the cubic box and the spacing between the grid points are selected in such a way that as many ''physical'' k vectors as possible will contribute to the calculation of the proper polarizability. By the term ''physical'' vectors we mean k vectors for which we have $|\mathbf{k}+\mathbf{q}|>|\mathbf{k}_F|$ and $|\mathbf{k}|<|\mathbf{k}_F|$, so that these k vectors correspond to a forward-going electron-hole pair; or $|\mathbf{k}+\mathbf{q}|<|\mathbf{k}_F|$ and $|\mathbf{k}|>|\mathbf{k}_F|$, so that these k vectors correspond to a backward-going electron-hole pair.

As seen in Eq. (15), we have to construct the matrices F^{-1} and W. The construction of the inverse free electron-hole propagator matrix is trivial. The free electron-hole propagator matrix F is diagonal in k space and therefore its inverse is also diagonal. The matrix elements of the inverse free electron-hole propagator are of the form

$$F^{-1}_{\mathbf{kk}'}=V(f(\mathbf{k})-f(\mathbf{k}+\mathbf{q}))[E(\mathbf{k})-E(\mathbf{k}+\mathbf{q})+i\eta]\delta_{\mathbf{kk}'}. \tag{16}$$

When constructing the screened Coulomb matrix W special care is needed for the selection of its dimensions and the arrangement of its matrix elements because as we explain below we have to Fourier transform this matrix. For $\mathbf{p}-\mathbf{k}=0$, the screened Coulomb interaction matrix diverges. We circumvent this problem by replacing the $W(\mathbf{p}-\mathbf{k}=0)$ value of the matrix with an average of W W_{av} over a sphere centered around $k=0$ with volume V_0 corresponding to one discrete k point:

$$W_{av}=\frac{4\pi}{V_0}\int_0^{k_0}dkk^2\epsilon^{-1}(k)v(k). \tag{17}$$

Here the volume V_0 is given by the expression

$$V_0=\frac{(2\pi)^3}{V}=\frac{4\pi k_0^3}{3}, \tag{18}$$

where k_0 is the radius of a sphere with volume V_0. Noting that for k approaching zero, $\epsilon^{-1}(k)$ is given by the expression

$$\lim_{k\to 0}\epsilon^{-1}(k)=Ak^2, \tag{19}$$

Eq. (17) takes the form

$$W_{av}=4\pi e^2A. \tag{20}$$

This substitution exploits ideas similar to those used by Godby, Schlüter, and Sham.[45]

Upon completion of the construction of the matrices F^{-1} and W the next step is the inversion of the matrix $F^{-1}-W$. The straightforward inversion of the matrix $F^{-1}-W$, although the most easily implemented, is not recommended because it scales as N^3, where N is the number of the physical vectors. By employing this approach, one would be forced to use a small number of physical vectors and there-

fore the accuracy of the calculations will be limited. Instead we use an iterative method for the inversion that scales better with respect to the number of physical vectors, so that we can easily converge results with respect to the number of physical vectors. Specifically, we use an iterative method to solve $A|x\rangle=|\Phi\rangle$, where we have $A=F^{-1}-W$. Note that $W_{\mathbf{pk}}$ depends only on the difference $\mathbf{p}-\mathbf{k}$. This means that if we Fourier transform W with respect to $\mathbf{k}$, the resulting matrix $\tilde{W}$ is diagonal in ''real space,'' which is a space in which the coordinate is the relative electron-hole separation. Hence, to act with the W matrix on some vector $|y\rangle$ we may Fourier transform $|y\rangle$ to real space, multiply by $\tilde{W}$, and Fourier transform the result back to k space. By employing this procedure, we are able to work with all physical quantities into convenient forms. This not only speeds up the calculation immensely, but also allows calculations in which a much larger number of physical wave vectors are considered, and the resulting convergence with respect to the number of physical wave vectors can be made fully satisfactory.

B. Jellium with a gap

Our choice of jellium with a gap or insulating jellium, as introduced by Levine and Louie,[46] is a two-parameter model. In addition to the electron gas parameter r_s, the gap is given by $\lambda\omega_F=E_{gap}/\hbar$. The main hypothesis is that the imaginary part of the model dielectric function that describes the system is

$$\text{Im}\ \epsilon_{LL}(\mathbf{q},\omega)=\begin{cases}\text{Im}\ \epsilon_L(\mathbf{q},\omega_-), & |\omega|\geqslant\lambda\omega_F\\ 0, & |\omega|<\lambda\omega_F.\end{cases} \tag{21}$$

Here ϵ_{LL} is the Levine-Louie model dielectric function, ϵ_L is the Lindhard dielectric function, $\omega_F=q_F^2/2$ is the Fermi frequency, and we have $\omega_-^2=\omega^2-(\lambda\omega_F)^2$. The sign of ω_- is taken to be the same as that of ω. The Levine-Louie model dielectric function is homogeneous, isotropic, has an analytic representation, and obeys causality and particle-number conservation.

The calculation of the static local-field factor for the case of jellium with a gap is almost identical with that of the gapless jellium, described in the preceding section, except for two modifications. First, the free electron-hole propagator matrix is given by the following expression:

$$F_{\mathbf{kk}'}=\frac{1}{V}\frac{f(\mathbf{k})-f(\mathbf{k}+\mathbf{q})}{\pm\sqrt{[E(\mathbf{k})-E(\mathbf{k}+\mathbf{q})]^2+(\lambda\omega_F)^2}+i\eta}\delta_{\mathbf{kk}'}, \tag{22}$$

where the upper and lower signs are to be used to mimic the sign of $E(\mathbf{k})-E(\mathbf{k}+\mathbf{q})$. Second, the Coulomb interaction is screened by the static Levine-Louie dielectric function given by

$$\epsilon_{LL}(\mathbf{q},0)=1+\frac{2}{q_Fa_0\pi}\left(\frac{1}{Q^2}-\frac{\lambda}{2Q^3}\times\left[\tan^{-1}\frac{2Q+Q^2}{\lambda}+\tan^{-1}\frac{2Q-Q^2}{\lambda}\right]+\left[\frac{\lambda^2}{8Q^5}+\frac{1}{2Q^3}-\frac{1}{8Q}\right]\ln\left[\frac{\lambda^2+(2Q+Q^2)^2}{\lambda^2+(2Q-Q^2)^2}\right]\right), \tag{23}$$

where we have $Q=q/q_F$.

For the determination of the parameter λ for a specific material, the static long-wavelength limit of the dielectric function

$$\epsilon_{LL}(0)=1+\left(\frac{\omega_p}{\lambda\omega_F}\right)^2 \tag{24}$$

is matched to the values available from experiment, where ω_p is the plasma frequency.

III. DISCUSSION OF RESULTS

In this section we will present our results for the static local-field factor for the case where the forward- and backward-going electron-hole pairs are coupled, and for the case where they are not coupled.

A. Jellium

In Fig. 4, the static local-field factor of jellium, $G(|\mathbf{q}|)$, is given for different values of r_s. The values of r_s used are 2.07, 3.25, 3.93, and 4.86, which correspond to the free-electron densities found in Al, Li, Na, and K, respectively. The forward- and backward-going electron-hole pairs are coupled. In this case, the main characteristics of the local-field factor are a parabolic region from 0 to $2|\mathbf{q}_F|$, a region consisting of a linear and a parabolic part from $2|\mathbf{q}_F|$ to $3.5|\mathbf{q}_F|$, and a cusp at $|\mathbf{q}|=2|\mathbf{q}_F|$. By writing the local-field factor as $G(|\mathbf{q}|)=a_0+a_1|\mathbf{q}|+a_2|\mathbf{q}|^2$ we are able to determine the parameters a_0, a_1, and a_2. The values of these parameters are given in Table I. At this point we have to emphasize that the small $|\mathbf{q}|$ region is purely parabolic for all the results we present in this paper. Because of the fact that we fit our data, for the small $|\mathbf{q}|$ region, with a second degree polynomial, a linear and a constant term appear for $G(|\mathbf{q}|)$. The coefficients of the linear and the constant term are negligible compared to the coefficients of the parabolic term and therefore are not taken into consideration. The results obtained by the diffusion Monte Carlo calculation of Moroni, Ceperley, and Senatore[47] indicate that $G(|\mathbf{q}|)$ is almost completely given by its asymptotes, and that it is reproduced quite accurately by the local-density approximation of density-functional theory for $|\mathbf{q}|\leqslant 2|\mathbf{q}_F|$. The asymptotic behavior of the static local-field factor of jellium is parabolic for both the small[47] and large[48] $|\mathbf{q}|$ regions.

Besides the fact that our results indicate that the region from $2|\mathbf{q}_F|$ to $3.5|\mathbf{q}_F|$ consists of a linear and a parabolic part, something which we believe comes from the fact that

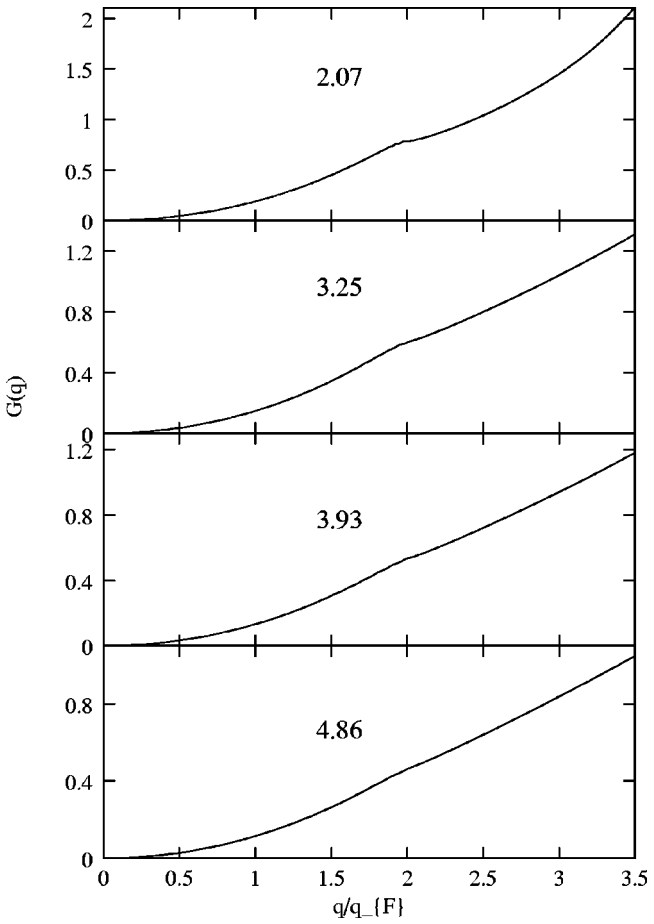

FIG. 4. Static local-field factor of gapless jellium for different values of r_s when the forward- and backward-going electron-hole pairs are coupled.

we sum only a specific subset of diagrams representing the interaction between the electron and the hole, another difference with the results of Moroni *et al.* is that our local-field factor decreases with increasing r_s. The explanation for this fact could be that in RPA, screening is larger for smaller values of r_s. This means that the screening hole spends more time in the vicinity of the electron. Therefore W, the interaction between the electron and the hole, is larger for smaller

TABLE I. Values of the expansion coefficients of the static local-field factor of gapless jellium in terms of $|\mathbf{q}|$ for different values of r_s when the forward- and backward-going electron-hole pairs are coupled.

r_s	Energy range	a_0	a_1	a_2
2.07	$0\rightarrow 2$			0.2178
	$2\rightarrow 3.5$	1.7646	−1.2567	0.3849
3.25	$0\rightarrow 2$			0.1604
	$2\rightarrow 3.5$	0.0789	0.1293	0.0637
3.93	$0\rightarrow 2$			0.1398
	$2\rightarrow 3.5$	−0.0251	0.1834	0.0460
4.86	$0\rightarrow 2$			0.1190
	$2\rightarrow 3.5$	−0.1112	0.2231	0.0309

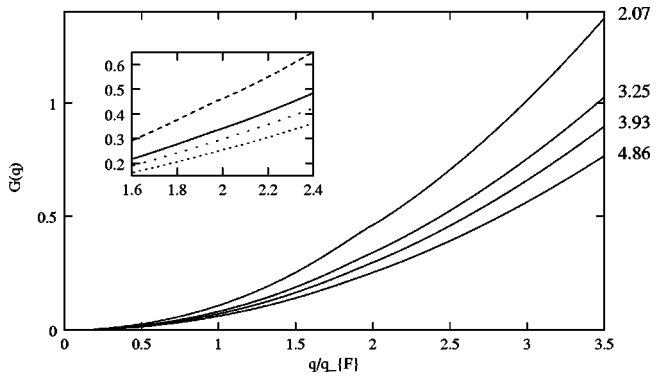

FIG. 5. Static local-field factor of gapless jellium for different values of r_s when the forward- and backward-going electron-hole pairs are not coupled.

r_s and therefore the local-field factor is larger. If all the exchange and correlation effects are taken into account more carefully, like in the calculation of Moroni *et al.*, the local-field factor has to increase with increasing r_s because of the exchange and correlation of the screening holes, which we do not take into consideration in our calculation. A comparison of the values of the local-field factor of our calculation and the calculation of Moroni *et al.* for very similar values of r_s and $|\mathbf{q}|$ is given in Table II. The values of $G(|\mathbf{q}|)$ are in reasonable agreement.

Concerning the cusp observed at $|\mathbf{q}|=2|\mathbf{q}_F|$, there is not a consensus in the literature whether this is an actual characteristic of the static local field of jellium or it is an artifact of the different approximations used to calculate $G(|\mathbf{q}|)$. The static $G(|\mathbf{q}|)$ of Brosens, Devreese, and Lemmens,[28–32] obtained through a dynamical-exchange decoupling in the equation of motion for the Wigner distribution function, clearly exhibits this cusp. Brosens, Devreese, and Lemmens attribute the cusp of the static local-field factor to the behavior of the dynamical local-field factor $G(\mathbf{q},\omega)$.[29] They proved that $G(\mathbf{q},\omega)$ has a logarithmic singularity at the frequencies $|\omega|=\hbar||\mathbf{q}|^2/2-|\mathbf{q}||\mathbf{q}_F||/m$. The two parabolas $\omega_1=\hbar(|\mathbf{q}|^2/2-|\mathbf{q}||\mathbf{q}_F|)/m$ and $\omega_2=\hbar(|\mathbf{q}||\mathbf{q}_F|-|\mathbf{q}|^2/2)$ intersect at $|\mathbf{q}|=2|\mathbf{q}_F|$ and $\omega=0$. At the point of intersection both

TABLE II. Comparison of the values of the static local-field factor of this work and the work of Moroni *et al.* (Ref. 47).

This work $r_s=2.07$ q/q_F		Moroni *et al.* $r_s=2.00$ q/q_F	
1.02	0.20	1.01	0.25(1)
1.10	0.23	1.08	0.28(2)
1.51	0.45	1.51	0.64(2)
1.61	0.52	1.61	0.77(1)
1.80	0.66	1.81	0.84(1)
2.00	0.78	2.01	0.90(7)
2.14	0.83	2.15	0.99(5)
2.41	0.98	2.42	1.04(12)
2.70	1.19	2.69	1.09(10)
3.02	1.47	3.02	1.18(9)

TABLE III. Values of the expansion coefficients of the static local-field factor of gapless jellium in terms of $|\mathbf{q}|$ for different values of r_s when the forward- and backward-going electron-hole pairs are not coupled.

r_s	Energy range	a_0	a_1	a_2
2.07	$0\rightarrow 2$			0.1258
	$2\rightarrow 3.5$	0.0584	-0.0326	0.1166
3.25	$0\rightarrow 3.5$			0.0824
3.93	$0\rightarrow 3.5$			0.0723
4.86	$0\rightarrow 3.5$			0.0620

singularities cancel each other. The cancellation of the two logarithmic singularities has as a result the appearance of a cusped structure in the static local-field factor. The cusp is also present in the Utsumi-Ichimaru model for the local-field factor[49,50] and by the calculations of Farid *et al.*,[51] who use the Utsumi-Ichimaru model as their starting point. The cusp in all these calculations, including ours, is substantially small compared to that obtained by the calculations of Brosens, Devreese, and Lemmens. Holas *et al.*,[52] using first-order perturbation theory in the Coulomb interaction, calculated the proper polarizability and consequently the static local-field factor. Their results reproduced the cusp, but the authors attributed this feature to the use of only the first-order diagrams in the calculation of the proper polarizability. Holas *et al.* came to this conclusion after comparing their results with the ones obtained by Geldart and Taylor,[34] who used higher-order diagrams for the calculation of the proper polarizability and did not obtain any cusped structure. Based on the present results, we suggest that the cusp is a mathematical feature of the static local-field factor, as it is defined in this work, as argued by Brosens, Devreese, and Lemmens.[29]

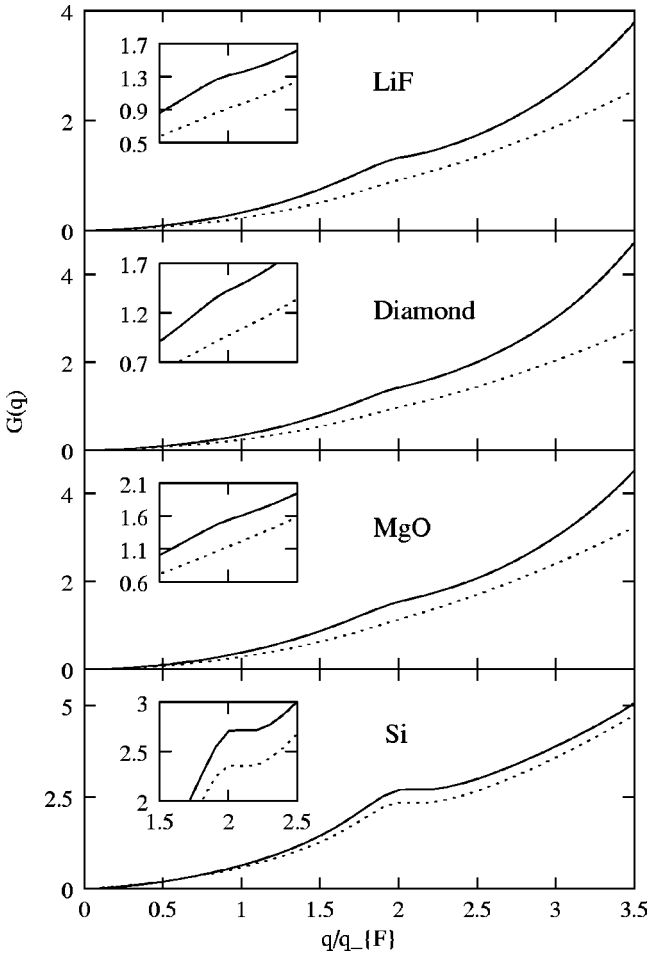

FIG. 6. Static local-field factor of jellium with a gap for different values of r_s and λ when both forward- and backward-going electron-hole pairs are coupled (solid curves) and not coupled (dashed curves).

TABLE IV. The values of r_s and λ used for the calculations of the static local-field factor of the insulating jellium.

Material	r_s	λ
LiF	1.4851	0.4050
MgO	1.5553	0.8294
Si	2.0060	0.4017
Diamond	1.3189	0.4982

In Fig. 5, we present the corresponding results for the static local-field factor, for different values of r_s, for the case when the forward- and backward-going electron-hole pairs are not coupled. The $2|\mathbf{q}_F|$ cusp is wiped out except for $r_s = 2.07$, where a tiny cusp is still present. When the $2|\mathbf{q}_F|$ cusp is eliminated, only one parabolic region is present, contrary to the fact that two different parabolic regions have to exist, one for small $\mathbf{q}$ and another for large $\mathbf{q}$. The main effect of the omission of the coupling is the suppression of the $2|\mathbf{q}_F|$ cusp. In Table III the coefficients of the expansion of $G(|\mathbf{q}|)$ with respect to $|\mathbf{q}|$ are given. Therefore it becomes evident that the coupling of the backward- to the forward-going electron hole pairs would be important for carrying out the most accurate calculations using the Bethe-Salpeter approach.

B. Jellium with a gap

In Fig. 6, we present the results for the static local-field factor of insulating jellium for the case where both types of electron-hole pairs are either coupled (solid line) or not

TABLE V. Values of the expansion coefficients of the static local-field factor of jellium with a gap in terms of $|\mathbf{q}|$ for different values of r_s when the forward- and backward-going electron-hole pairs are coupled.

Material	Energy range	a_0	a_1	a_2
LiF	$0\rightarrow 2$			0.3565
	$2\rightarrow 3.5$	3.9422	-2.9728	0.8334
MgO	$0\rightarrow 2$			0.3975
	$2\rightarrow 3.5$	4.5082	-3.4144	0.9739
Si	$0\rightarrow 2$			0.7449
	$2\rightarrow 3.5$	3.8986	-2.0660	0.6867
Diamond	$0\rightarrow 2$			0.3845
	$2\rightarrow 3.5$	5.2104	-4.1458	1.1402

TABLE VI. Values of the expansion coefficients of the static local-field factor of jellium with a gap in terms of $|\mathbf{q}|$ for different values of r_s when the forward- and backward-going electron-hole pairs are not coupled.

Material	Energy range	a_0	a_1	a_2
LiF	$0\rightarrow 2$			0.2399
	$2\rightarrow 3.5$	0.3734	-0.2020	0.2351
MgO	$0\rightarrow 3.5$			0.2468
Si	$0\rightarrow 2$			0.5619
	$2\rightarrow 3.5$	2.9557	-1.6488	0.6185
Diamond	$0\rightarrow 2$			0.2519
	$2\rightarrow 3.5$	0.2715	-0.1347	0.2411

coupled (dashed line). The calculations were done for the values of r_s and λ that correspond to MgO, Si, diamond, and LiF. These values of r_s and λ are given in Table IV. The main features of the results are the same as those of the gapless jellium presented in the preceding section. The local-field factor exhibits a cusp at $|\mathbf{q}|=2|\mathbf{q}_F|$ and is mainly characterized by one parabolic regime for $|\mathbf{q}|\leqslant 2|\mathbf{q}_F|$ and a regime for $|\mathbf{q}|\geqslant 2|\mathbf{q}_F|$ which consists of a linear and a parabolic part. The values of the expansion coefficients of $G(|\mathbf{q}|)$ in terms of $|\mathbf{q}|$ are given in Table V. For the jellium with a gap, the cusp at $2|\mathbf{q}_F|$ appears to be higher especially for the case of Si. For the case of Si the static local-field factor exhibits also a hump near $2|\mathbf{q}_F|$.

Finally, the static local-field factor is given for the case where the forward- and backward-going electron-hole pairs are not coupled. We see that for Si, diamond, and LiF, the $2|\mathbf{q}_F|$ cusp is still present, although it is smaller in size considerably compared to the case where both electron-hole pair types are coupled. For the case of MgO, the $2|\mathbf{q}_F|$ cusp is totally eliminated, and the static local-field factor is mainly characterized by one parabolic regime, which is qualitatively a very different result. The values of the expansion coefficients of $G(|\mathbf{q}|)$ in terms of $|\mathbf{q}|$ are given in Table VI. Therefore the main effect of the omission of the coupling between the two types of the electron-hole pairs is the suppression of the $2|\mathbf{q}_F|$ cusp. The elimination of the $2|\mathbf{q}_F|$ cusp depends on its height when both kinds of electron-hole pairs are coupled. If the cusp is sufficiently large, it will not disappear, and the static local-field factor will be characterized by two regimes, as it should be. On the other hand, if the cusp originally is not sufficiently large, it will be wiped out by the lack of coupling. This will lead to a static local-field factor characterized by only one parabolic regime.

IV. CONCLUSIONS

We presented the calculation of the static local-field factor of jellium using the Bethe-Salpeter equation. We only considered diagrams where the electron-hole pair interact via a statically screened Coulomb interaction and we summed these diagrams to infinite order. In our calculation of the static local-field factor we coupled the forward- and backward-going electron-hole pairs. We compared these results with the corresponding results obtained when the coupling is omitted, and we conclude that the coupling of both kinds of electron-hole pairs is relevant for the most accurate calculation using the Bethe-Salpeter equation. The main effect of the omission of coupling between the forward- and backward-going electron-hole pairs is the suppression of the $2|\mathbf{q}_F|$ cusp. The elimination of the $2|\mathbf{q}_F|$ cusp depends on its height when both kinds of electron-hole pairs are coupled. If the cusp is sufficiently large, it will not disappear, and the static local-field factor will be characterized by two regimes, as it should be. On the other hand, if the cusp originally is not sufficiently large, it will be wiped out by the neglect of coupling. This will lead to a static local-field factor characterized by only one parabolic regime. This might have implications for the Bethe-Salpeter calculations in real solids. Another interesting feature of our calculation is the high accuracy combined with the speed of calculation. This is achieved by the conversion of the relevant matrices into convenient forms and the use of an iterative inversion approach.

ACKNOWLEDGMENTS

The authors would like to thank Valerio Olevano, Eric K. Chang, J. A. Soininen, and Dyutiman Das for useful discussions. A. T. is very grateful for the hospitality provided by NIST during the fall of 2001. This material is based upon work supported by the U.S. Department of Energy, Division of Material Sciences under Grant No. DEFG02-91ER45439, through the Frederick Seitz Materials Research Laboratory at the University of Illinois at Urbana-Champaign.

[1] S. Albrecht, L. Reining, R. Del Sole, and G. Onida, Phys. Rev. Lett. **80**, 4510 (1998).
[2] L.X. Benedict, E.L. Shirley, and R.B. Bohn, Phys. Rev. B **57**, R9385 (1998).
[3] L.X. Benedict and E.L. Shirley, Phys. Rev. B **59**, 5441 (1999).
[4] G. Onida, L. Reining, R.W. Godby, R. Del Sole, and W. Andreoni, Phys. Rev. Lett. **75**, 818 (1995).
[5] M. Rohlfing and S.G. Louie, Phys. Rev. Lett. **81**, 2312 (1998).
[6] J.A. Soininen and E.L. Shirley, Phys. Rev. B **61**, 16 423 (2000).
[7] G. Onida, L. Reining, and A. Rubio, Rev. Mod. Phys. **74**, 601 (2002).
[8] V. Olevano and L. Reining, Phys. Rev. Lett. **86**, 5962 (2001).
[9] J. Stiebling, Z. Phys. B **31**, 355 (1978).
[10] D.R. Penn, Phys. Rev. **128**, 2093 (1962).
[11] J. Hubbard, Proc. R. Soc. London, Ser. A **243**, 336 (1957).
[12] L.J. Sham, Proc. R. Soc. London, Ser. A **283**, 33 (1965).
[13] W.M. Shyu and G.D. Gaspari, Phys. Rev. **163**, 667 (1967).
[14] W.M. Shyu and G.D. Gaspari, Phys. Rev. **170**, 687 (1968).
[15] D.J.W. Geldart and S.H. Vosko, Can. J. Phys. **44**, 2137 (1966).
[16] K.S. Singwi, M.P. Tosi, R.H. Land, and A. Sjölander, Phys. Rev. **176**, 589 (1968).

[17] K.S. Singwi, A. Sjölander, M.P. Tosi, and R.H. Land, Phys. Rev. B **1**, 1044 (1970).
[18] P. Vashishta and K.S. Singwi, Phys. Rev. B **6**, 875 (1972).
[19] J.S. Vaishya and A.K. Gupta, Phys. Rev. B **7**, 4300 (1973).
[20] A.K. Gupta and K.S. Singwi, Phys. Rev. B **15**, 1801 (1977).
[21] L. Kleinman, Phys. Rev. **160**, 585 (1967).
[22] L. Kleinman, Phys. Rev. **172**, 383 (1968).
[23] D.C. Langreth, Phys. Rev. **181**, 753 (1969).
[24] J.W.F. Woo and S.S. Jha, Phys. Rev. B **3**, 87 (1971).
[25] S.S. Jha, K.K. Gupta, and J.W.F. Woo, Phys. Rev. B **4**, 1005 (1971).
[26] A.K. Rajagopal and K.P. Jain, Phys. Rev. A **5**, 1475 (1972).
[27] A.K. Rajagopal, Phys. Rev. A **6**, 1239 (1972).
[28] F. Brosens, L.F. Lemens, and J.T. Devreese, Phys. Status Solidi B **74**, 45 (1976).
[29] F. Brosens, J.T. Devreese, and L.F. Lemmens, Phys. Status Solidi B **80**, 99 (1977).
[30] F. Brosens, L.F. Lemmens, and J.T. Devreese, Phys. Status Solidi B **81**, 551 (1977).
[31] J.T. Devreese, F. Brosens, and L.F. Lemmens, Phys. Rev. B **21**, 1349 (1980).
[32] F. Brosens, J.T. Devreese, and L.F. Lemmens, Phys. Rev. B **21**, 1363 (1980).
[33] D.J.W. Geldart and R. Taylor, Can. J. Phys. **48**, 155 (1970).
[34] D.J.W. Geldart and R. Taylor, Can. J. Phys. **48**, 167 (1970).
[35] D.J.W. Geldart, Can. J. Phys. **45**, 3139 (1967).
[36] F. Toigo and T.O. Woodruff, Phys. Rev. B **2**, 3958 (1970).
[37] F. Toigo and T.O. Woodruff, Phys. Rev. B **4**, 371 (1971).
[38] L. Hedin and S. Lundqvist, Solid State Phys. **23**, 1 (1969).
[39] A.W. Overhauser, Phys. Rev. B **3**, 1888 (1971).
[40] L.J. Sham, Phys. Rev. B **7**, 4357 (1973).
[41] K.S. Singwi and M.P. Tosi, Solid State Phys. **36**, 177 (1981).
[42] P. Hohenberg and W. Kohn, Phys. Rev. **136**, B864 (1964).
[43] W. Kohn and L.J. Sham, Phys. Rev. **140**, A1133 (1965).
[44] See, for instance, A. Fetter and D. Walecka, *Quantum Theory of Many-Particle Systems* (McGraw-Hill, San Francisco, 1971).
[45] R.W. Godby, M. Schlüter, and L.J. Sham, Phys. Rev. B **37**, 10 159 (1988).
[46] Z.H. Levine and S.G. Louie, Phys. Rev. B **25**, 6310 (1982).
[47] S. Moroni, D.M. Ceperley, and G. Senatore, Phys. Rev. Lett. **75**, 689 (1995).
[48] A. Holas, in *Strongly Coupled Plasma Physics*, edited by F.J. Rogers and H.E. DeWitt (Plenum, New York, 1987), p. 463.
[49] K. Utsumi and S. Ichimaru, Phys. Rev. B **22**, 5203 (1980).
[50] S. Ichimaru, Rev. Mod. Phys. **54**, 1017 (1982).
[51] B. Farid, V. Heine, G.E. Engel, and I.J. Robertson, Phys. Rev. B **48**, 11 602 (1993).
[52] A. Holas, P.K. Aravind, and K.S. Singwi, Phys. Rev. B **20**, 4912 (1979).